ISSN 1063-7761, Journal of Experimental and Theoretical Physics, 2017, Vol. 124, No. 2, pp. 295–303. © Pleiades Publishing, Inc., 2017.
Original Russian Text © V.I. Zinenko, M.S. Pavlovskii, 2017, published in Zhurnal Eksperimental'noi i Teoreticheskoi Fiziki, 2017, Vol. 151, No. 2, pp. 346–355.

ORDER, DISORDER, AND PHASE TRANSITION IN CONDENSED SYSTEM

Thermodynamics of Spin Ice in Staggered and Direct (along the [111] Axis) Fields in the Cluster Approximation

V. I. Zinenko* and M. S. Pavlovskii

Kirensky Institute of Physics, Siberian Branch, Russian Academy of Sciences, Krasnoyarsk, 660036 Russia

**e-mail: zvi@iph.krasn.ru*

Received July 18, 2016

Abstract—We have analyzed the low-temperature thermodynamic properties of spin ice in the staggered and direct (acting along the [111] axis) fields for rare-earth oxides with the chalcolamprite structure and general formula $Re_2^{3+}Me_2^{4+}O_7^{2-}$. Calculations have been performed in the cluster approximation. The results have been compared with experimental temperature dependences of heat capacity and entropy for $Dy_2Ti_2O_7$ compound for different values of the external field in the [111] direction. The experimental data and calculated results have also been compared for the $Pr_2Ru_2O_7$ compound with the antiferromagnetic ordering of magnetic moments of ruthenium ions, which gives rise to the staggered field acting on the system of rare-earth ions. The calculated temperature dependences of heat capacity and entropy are in good agreement with experimental data.

DOI: 10.1134/S1063776117020182

1. INTRODUCTION

The thermodynamic properties of geometrically frustrated magnetic systems have attracted the attention of researchers for many decades. The ground state in these systems has a high degree of degeneracy, which leads to residual entropy at $T = 0$ and often results in the peculiar behavior of thermodynamic quantities in the low-temperature range. After the discovery of the spin ice state in compounds with the chalcolamprite structure [1, 2], the interest in geometrically frustrated magnets increases considerably, and a large number of publications have been devoted to analyzing the properties of spin ice (see, e.g., reviews [3, 4]).

In compounds with chalcolamprite structures containing rare-earth ions, these ions form a 3D network of tetrahedrons connected at vertices. Since the spins of *f* electrons of rare-earth elements have a large magnetic moment, they can be treated as classical variables, and their behavior at low temperatures can be described as an Ising doublet directed along the axis connecting the center of a tetrahedron with its vertex. Geometrical frustration is caused by noncollinearity of the crystal field and effective magnetic interaction, as well as by the fact that the directions of axes in the Ising doublet in a unit cell are fixed and different. As a result, there are six possible configurations for each tetrahedron with the same energy, which corresponds to the free energy minimum; therefore, the ground state of the system of magnetic moments of rare-earth ions is infinitely degenerate.

The low-temperature physics of spin ice in the absence and in the presence of an external magnetic field has been studied experimentally for many compounds with the chalcolamprite structure [1–4].

A theoretical analysis of the effect of an external magnetic field on the thermodynamic properties of spin ice was carried out both numerically using the Monte Carlo method and analytically on the Bethe lattice in the Bethe–Peierls approximation [5, 6]. However, among crystals with the chalcolamprite structure containing rare-earth ions ($R_2^{3+}B_2^{4+}O_7$, where R stands for a rare-earth element), there are compounds in which the tetravalent metal B^{4+} has a nonzero magnetic moment. It has been found experimentally that, e.g., compounds $Pr_2Ru_2O_7$ [7], $R_2Ru_2O_7$ (R = Gd–Yb) [8], and $Ho_2Os_2O_7$ [9] exhibit the antiferromagnetic phase transition in the magnetic system of the B^{4+} ions at temperatures on the order of tens of kelvins.

This study aims at analyzing the effect of antiferromagnetic ordering in the system of magnetic B^{4+} ions on the thermodynamic properties of spin ice in the magnetic system of rare-earth ions on the chalcolamprite lattice.

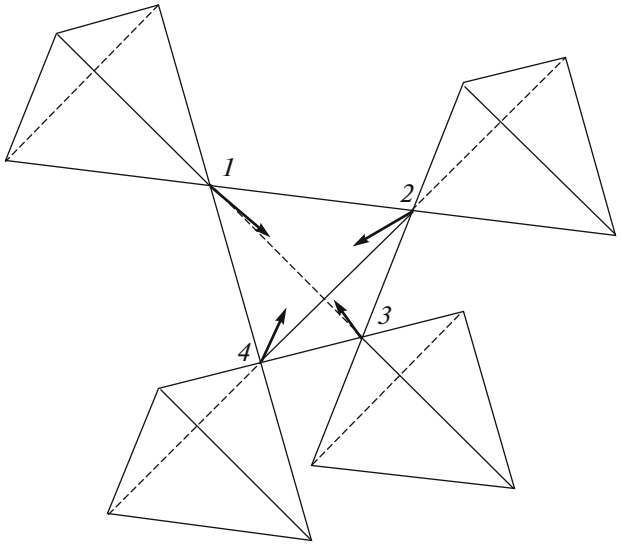

Fig. 1. Fragment of the chalcolamprite structure; tetrahedrons of rare-earth ions with connected vertices and the vectors of the direction of the Ising doublet are indicated.

2. FREE ENERGY AND EXPRESSIONS FOR MEAN MAGNETIC MOMENTS IN THE FOUR-PARTICLE CLUSTER APPROXIMATION

We will consider only the magnetic system of rare-earth ions and the existence of antiferromagnetic ordering in the system of B^{4+} ions will be taken into account as the field S acting on the magnetic moments of rare-earth ions. Figure 1 shows a fragment of the chalcolamprite lattice of the rare-earth ions and the vectors indicating the directions of an Ising doublet in a unit cell.

The ground state of the system of magnetic ions of a rare-earth element can be treated as a vertex with one of 16 possible configurations of the spins of a tetrahedron. The vertex configurations of these spins are shown in Fig. 2. Six configurations v_1-v_6 allowed by the ice rule (i.e., two-in, two-out) have the same energy that is set as zero. Eight configurations v_7-v_{14} (four with a positive magnetic charge and four with a negative magnetic charge) also possess the same energy ε. For simplicity, we will henceforth assume that the energy of doubly charged configurations (v_{15} and v_{16}) is $\omega = 2\varepsilon$.

We set $\sigma_i^z = \pm 1$ for two possible directions of the magnetic moment of a rare-earth ion (inward or outward relative to the tetrahedron). Then, the model Hamiltonian can be written as the Hamiltonian in the Ising model with the interaction of spins adjoining each vertex (see, e.g., [10]).

To take into account the staggered field S exerted on the magnetic moments of the rare-earth ion by antiferromagnetically ordered B^{4+} ions, we consider

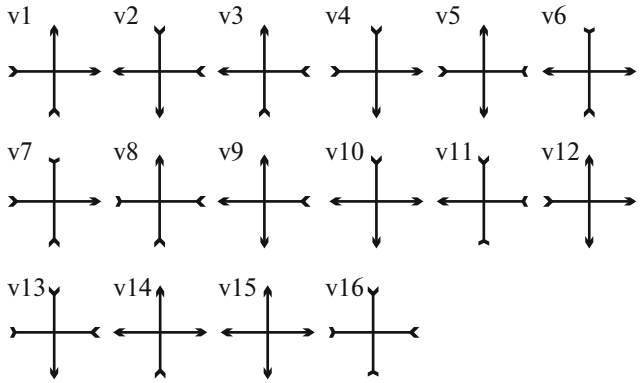

Fig. 2. Vertex configurations of the spins of a tetrahedron of rare-earth ions.

the peculiarities in the structure of chalcolamprite. In this structure, the system of B^{4+} ions also forms the 3D network of tetrahedrons connected at the vertices, so that each rare-earth ion has six nearest neighboring B^{4+} ions. Figure 3 shows a fragment of the structure of chalcolamprite containing a tetrahedron of R^{3+} ions with each such ion surrounded by the nearest B^{4+} ions. It can be seen from the figure that, in the case of antiferromagnetic ordering in the system of B^{4+} ions, two R^{3+} ions in the tetrahedron (denoted by *1* and *2* in Fig. 3) experience the action of total field S with the "—" sign, while total field S with the "+" sign acts on the other two ions (denoted by *3* and *4* in Fig. 3).

To describe the thermodynamic properties of the model, we will use the cluster approximation and consider the simplest cluster of four spins analogously to that used in the theory of KDP-type ferroelectrics [11].

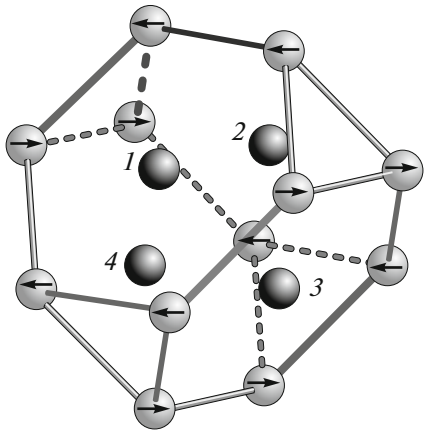

Fig. 3. Fragment of the chalcolamprite structure containing a tetrahedron of Re^{3+} ions (dark balls) and the nearest surrounding of each R^{3+} ion by B^{4+} ions (light balls). Black arrows show the directions of magnetic moments of B^{4+} ions in the case of antiferromagnetic ordering.

In this approximation, with allowance for the action of the staggered field shown in Fig. 3, the mean energy for a vertex has the form

$$E = \langle \mathcal{H}_{\rm cl}\rangle - \frac{1}{2}\sum_{i=1}^{4}\langle \mathcal{H}_i\rangle = \langle \mathcal{H}_{\rm int} - \varphi_1\sigma_1^z - \varphi_2\sigma_2^z - \varphi_3\sigma_3^z - \varphi_4\sigma_4^z - S(\sigma_1^z + \sigma_2^z) + S(\sigma_3^z + \sigma_4^z) - H(\sigma_1^z - \sigma_2^z - \sigma_3^z - \sigma_4^z)\rangle - \frac{1}{2}\langle(2\varphi_1 + S + H)\sigma_1^z\rangle - \frac{1}{2}\langle(2\varphi_2 + S - H)\sigma_2^z\rangle - \frac{1}{2}\langle(2\varphi_3 - S - H)\sigma_3^z\rangle - \frac{1}{2}\langle(2\varphi_4 - S - H)\sigma_4^z\rangle, \quad (1)$$

where $\mathcal{H}_{\rm int}$ includes the interaction of spins *1*, *2*, *3*, and *4* with one another; and φ_i is the field exerted on the *i*th spin by each adjoining vertex. We included external magnetic field H, which acts in the [111] direction, which induces the state of magnetic monopoles, into expression (1) to compare the result with experimental data on the low-temperature thermodynamics in an external field in rare-earth oxides with the chalcolamprite structure.

To calculate the mean value of energy (1) in the cluster approximation, density matrices ρ_k of the *k*th cluster are described by the expression $\rho_k = \text{const}\exp(-\beta\mathcal{H}_k)$, where $\mathcal{H}_k$ is the cluster ($\mathcal{H}_{\rm cl}$) and one-particle ($\mathcal{H}_i$) Hamiltonians defined in expression (1) [11], and $\beta = 1/T$ ($k_{\rm B} = 1$). The free energy can be determined by integrating the relation $E = \partial(\beta F)/\partial\beta$ over β as follows:

$$\beta F = -\ln Z_{\rm cl} + \frac{1}{2}\ln Z_1 + \frac{1}{2}\ln Z_2 + \frac{1}{2}\ln Z_3 + \frac{1}{2}\ln Z_4. \quad (2)$$

Here, $Z_{\rm cl}$ and Z_i are the cluster and one-particle partition functions as follows:

$$\begin{aligned} Z_{\rm cl} = 2[&\cosh\beta(\varphi_1 + \varphi_2 + \varphi_3 + \varphi_4 - 2H) \\ &+\cosh\beta(\varphi_1 - \varphi_2 - \varphi_3 + \varphi_4 + 2H) \\ &+\cosh\beta(\varphi_1 + \varphi_2 - \varphi_3 - \varphi_4 + 4S + 2H) \\ &+e^{-\beta\varepsilon}(\cosh\beta(\varphi_1 + \varphi_2 - \varphi_3 + \varphi_4 + 2S) \\ &+\cosh\beta(\varphi_1 + \varphi_2 + \varphi_3 - \varphi_4 + 2S) \\ &+\cosh\beta(\varphi_1 - \varphi_2 - \varphi_3 - \varphi_4 + 2S + 4H) \\ &+\cosh\beta(\varphi_1 - \varphi_2 + \varphi_3 + \varphi_4 - 2S)) \\ &+e^{-2\beta\varepsilon}\cosh\beta(\varphi_1 - \varphi_2 + \varphi_3 - \varphi_4 + 2H)], \\ Z_1 = 2\cosh\beta(2\varphi_1 + S + H), \\ Z_2 = 2\cosh\beta(2\varphi_2 + S - H), \\ Z_3 = 2\cosh\beta(2\varphi_3 - S - H), \\ Z_4 = 2\cosh\beta(2\varphi_4 - S - H). \end{aligned} \quad (3)$$

Fields φ_i can be determined from the condition $\partial F/\partial\varphi_i = 0$ of the free energy minimum and can be found from the following system of equations:

$$\begin{aligned} &\sinh\beta(-\varphi_1 + \varphi_2 + \varphi_3 + \varphi_4 - S - 3H) \\ &+\sinh\beta(-\varphi_1 - \varphi_2 - \varphi_3 + \varphi_4 + S + H) \\ &+\sinh\beta(-\varphi_1 + \varphi_2 - \varphi_3 - \varphi_4 + 3S + H) \\ &+e^{-\beta\varepsilon}(\sinh\beta(-\varphi_1 + \varphi_2 - \varphi_3 + \varphi_4 + S - H) \\ &+\sinh\beta(-\varphi_1 + \varphi_2 + \varphi_3 - \varphi_4 + S - H) \\ &+\sinh\beta(-\varphi_1 - \varphi_2 - \varphi_3 - \varphi_4 + S + 3H) \\ &+\sinh\beta(-\varphi_1 - \varphi_2 + \varphi_3 + \varphi_4 - 3S - H)) \\ &+e^{-2\beta\varepsilon}\sinh\beta(-\varphi_1 - \varphi_2 + \varphi_3 - \varphi_4 - S + H) = 0, \end{aligned} \quad (4)$$

$$\begin{aligned} &\sinh\beta(\varphi_1 - \varphi_2 + \varphi_3 + \varphi_4 - S - H) \\ &-\sinh\beta(\varphi_1 + \varphi_2 - \varphi_3 + \varphi_4 + S + H) \\ &+\sinh\beta(\varphi_1 - \varphi_2 - \varphi_3 - \varphi_4 + 3S + 3H) \\ &+e^{-\beta\varepsilon}(\sinh\beta(\varphi_1 - \varphi_2 - \varphi_3 + \varphi_4 + S + H) \\ &+\sinh\beta(\varphi_1 - \varphi_2 + \varphi_3 - \varphi_4 + S + H) \\ &-\sinh\beta(\varphi_1 + \varphi_2 - \varphi_3 - \varphi_4 + 3S + 3H) \\ &-\sinh\beta(\varphi_1 + \varphi_2 + \varphi_3 + \varphi_4 - S - H)) \\ &-e^{-2\beta\varepsilon}\sinh\beta(\varphi_1 + \varphi_2 + \varphi_3 - \varphi_4 + S + H) = 0, \end{aligned} \quad (5)$$

$$\begin{aligned} &\sinh\beta(\varphi_1 + \varphi_2 - \varphi_3 + \varphi_4 + S - H) \\ &-\sinh\beta(\varphi_1 - \varphi_2 + \varphi_3 + \varphi_4 - S + H) \\ &-\sinh\beta(\varphi_1 + \varphi_2 + \varphi_3 - \varphi_4 + 3S + H) \\ &-e^{-\beta\varepsilon}(\sinh\beta(\varphi_1 + \varphi_2 + \varphi_3 + \varphi_4 + S - H) \\ &-\sinh\beta(\varphi_1 + \varphi_2 - \varphi_3 - \varphi_4 + 3S + H) \\ &+\sinh\beta(\varphi_1 - \varphi_2 + \varphi_3 - \varphi_4 + S + 3H) \\ &-\sinh\beta(\varphi_1 - \varphi_2 - \varphi_3 + \varphi_4 - S + H)) \\ &+e^{-2\beta\varepsilon}\sinh\beta(\varphi_1 - \varphi_2 - \varphi_3 - \varphi_4 + S + 3H) = 0, \end{aligned} \quad (6)$$

$$\begin{aligned} &\sinh\beta(\varphi_1 + \varphi_2 + \varphi_3 - \varphi_4 + S - H) \\ &+\sinh\beta(\varphi_1 - \varphi_2 - \varphi_3 - \varphi_4 + S + 3H) \\ &-\sinh\beta(\varphi_1 + \varphi_2 - \varphi_3 + \varphi_4 + 3S + H) \\ &+e^{-\beta\varepsilon}(\sinh\beta(\varphi_1 + \varphi_2 - \varphi_3 - \varphi_4 + 3S + H) \\ &-\sinh\beta(\varphi_1 + \varphi_2 + \varphi_3 + \varphi_4 + S - H) \\ &-\sinh\beta(\varphi_1 - \varphi_2 - \varphi_3 + \varphi_4 + S + 3H) \\ &+\sinh\beta(\varphi_1 - \varphi_2 + \varphi_3 - \varphi_4 - S + H)) \\ &-e^{-2\beta\varepsilon}\sinh\beta(\varphi_1 - \varphi_2 + \varphi_3 + \varphi_4 - S + H) = 0. \end{aligned} \quad (7)$$

Mean values $\langle\sigma_i^z\rangle$ are defined by the expressions

$$\langle\sigma_1^z\rangle = \frac{2}{Z_{\rm cl}}[\sinh\beta(\varphi_1+\varphi_2+\varphi_3+\varphi_4-2H) + \sinh\beta(\varphi_1-\varphi_2-\varphi_3+\varphi_4+2H) + \sinh\beta(\varphi_1+\varphi_2-\varphi_3-\varphi_4+4S+2H) + e^{-\beta\varepsilon}(\sinh\beta(\varphi_1+\varphi_2-\varphi_3+\varphi_4+2S) + \sinh\beta(\varphi_1+\varphi_2+\varphi_3-\varphi_4+2S) + \sinh\beta(\varphi_1-\varphi_2-\varphi_3-\varphi_4+2S+4H) + \sinh\beta(\varphi_1-\varphi_2+\varphi_3+\varphi_4-2S)) + e^{-\beta\varepsilon}\sinh\beta(\varphi_1-\varphi_2+\varphi_3-\varphi_4+2H)], \quad (8)$$

$$\langle\sigma_2^z\rangle = \frac{2}{Z_{\rm cl}}[\sinh\beta(\varphi_1+\varphi_2+\varphi_3+\varphi_4-2H) - \sinh\beta(\varphi_1-\varphi_2-\varphi_3+\varphi_4+2H) + \sinh\beta(\varphi_1+\varphi_2-\varphi_3-\varphi_4+4S+2H) + e^{-\beta\varepsilon}(\sinh\beta(\varphi_1+\varphi_2-\varphi_3+\varphi_4+2S) + \sinh\beta(\varphi_1+\varphi_2+\varphi_3-\varphi_4+2S) - \sinh\beta(\varphi_1-\varphi_2-\varphi_3-\varphi_4+2S+4H) - \sinh\beta(\varphi_1-\varphi_2+\varphi_3+\varphi_4-2S)) - e^{-\beta\varepsilon}\sinh\beta(\varphi_1-\varphi_2+\varphi_3-\varphi_4+2H)], \quad (9)$$

$$\langle\sigma_3^z\rangle = \frac{2}{Z_{\rm cl}}[\sinh\beta(\varphi_1+\varphi_2+\varphi_3+\varphi_4-2H) - \sinh\beta(\varphi_1-\varphi_2-\varphi_3+\varphi_4+2H) - \sinh\beta(\varphi_1+\varphi_2-\varphi_3-\varphi_4+4S+2H) - e^{-\beta\varepsilon}(\sinh\beta(\varphi_1+\varphi_2-\varphi_3+\varphi_4+2S) - \sinh\beta(\varphi_1+\varphi_2+\varphi_3-\varphi_4+2S) + \sinh\beta(\varphi_1-\varphi_2-\varphi_3-\varphi_4+2S+4H) - \sinh\beta(\varphi_1-\varphi_2+\varphi_3+\varphi_4-2S)) + e^{-\beta\varepsilon}\sinh\beta(\varphi_1-\varphi_2+\varphi_3-\varphi_4+2H)], \quad (10)$$

$$\langle\sigma_4^z\rangle = \frac{2}{Z_{\rm cl}}[\sinh\beta(\varphi_1+\varphi_2+\varphi_3+\varphi_4-2H) + \sinh\beta(\varphi_1-\varphi_2-\varphi_3+\varphi_4+2H) - \sinh\beta(\varphi_1+\varphi_2-\varphi_3-\varphi_4+4S+2H) + e^{-\beta\varepsilon}(\sinh\beta(\varphi_1+\varphi_2-\varphi_3+\varphi_4+2S) - \sinh\beta(\varphi_1+\varphi_2+\varphi_3-\varphi_4+2S) - \sinh\beta(\varphi_1-\varphi_2-\varphi_3-\varphi_4+2S+4H) + \sinh\beta(\varphi_1-\varphi_2+\varphi_3+\varphi_4-2S)) - e^{-\beta\varepsilon}\sinh\beta(\varphi_1-\varphi_2+\varphi_3-\varphi_4+2H)]. \quad (11)$$

The entropy and specific heat are defined as

$$S_m = -\left.\frac{\partial F}{\partial T}\right|_{H=0}, \quad C_V = -T\left.\frac{\partial^2 F}{\partial T^2}\right|_{H=0}. \quad (12)$$

Expressions (2)–(12) describe the thermodynamics of the system.

3. RESULTS AND COMPARISON WITH EXPERIMENT

Above all, it should be noted that, in the zero field conditions ($S = H = 0$), system of equations (4)–(7) can be reduced to the following single equation for self-consistent field $\varphi = \varphi_1 = \varphi_2 = \varphi_3 = \varphi_4$:

$$\sinh(2\beta\varphi)[1 + e^{-2\beta\varepsilon} + 2e^{-\beta\varepsilon}\cosh(\beta\varphi)] = 0. \quad (13)$$

This equation has the single solution $\varphi = 0$ at all temperatures; i.e., in zero fields, the system of magnetic moments of rare-earth ions is infinitely degenerate at $T = 0$. It should also be noted that, if we exclude excited configurations with a magnetic charge (i.e., assume that $\varepsilon = \infty$), Eq. (2) leads to the following Polling result [12] for residual entropy: $F = -T\ln(3/2)$, $S_m = \ln(3/2)$.

Let us now consider the results obtained for nonzero values of fields S and H.

1. $S = 0$, $H \neq 0$.

The dependences of the specific heat, entropy, and mean values $\langle\sigma_i^z\rangle$ on dimensionless temperature $t = T/\varepsilon$ for different values of external field $h = H/\varepsilon$ are shown in Figs. 4–6 (the calculated values of heat capacity and entropy are given in the units of R, where $R = 8.31$ J/(mol K) is the universal gas constant, except for the cases when these values are compared with experimental data). For better visualization, the temperature dependences of the specific heat and entropy are shown in different figures for small and large values of field h.

For zero field h, the dependence for the specific heat has a broad anomaly at $t \approx 0.5$ (Fig. 4a) associated with the excitation of states with a magnetic charge (three inward spins and one outward spin). The ground state of the system for $h = 0$ is infinitely degenerate as noted above, which leads to residual entropy at $T = 0$ (Fig. 5a). For a nonzero value of h, six states of each tetrahedron (two inward spins and two outward spins), which have zero energy at $h = 0$, split into two states with energy $-2h$ and four states with energy $+2h$; for small values of field h, the system at $T = 0$ remains degenerate with a lower degree of degeneracy. In this case, the temperature dependence of heat capacity displays two anomalies (see Fig. 4a). The first anomaly at low temperatures is associated with the excitation of states with energy $2h$, while the peak of the second anomaly, which is associated with excitation of magnetically charges configurations, slightly increases. As the field increases to $h \approx 0.1$, the first

anomaly in the behavior of heat capacity shifts sharply towards higher temperatures and merges with the second broad anomaly (see Fig. 4a); beginning with fields $h \approx 0.2$, the peak of this anomaly decreases and is shifted towards higher temperatures (see Fig. 4b). In fields $h = 0.5–1.0$, the energies of the two states of spin ice and one of the magnetically charged states are close, which again leads to anomalous behavior of the heat capacity at low temperatures (Fig. 4c). In field $h \approx 0.1$, the ground state becomes a fully ordered magnetically charged state; this can be seen from the temperature dependences of mean values $\langle \sigma_i^Z \rangle$ in Fig. 6 and of entropy in Fig. 5b. In fields $h > 1$, the behavior of the heat capacity acquires an anomaly associated with the excitation of spin ice states from the ground magnetically charged state (see Fig. 4c). The case with $S = 0$ and $H \neq 0$ under investigation refers to compounds of rare-earth oxides with the chalcolamprite structure, in which the role of B^{4+} is played by a nonmagnetic ion. The low-temperature thermodynamics of spin ice under the action of field H in the [111] direction was investigated experimentally for several such compounds [13, 14]. To a certain extent, the temperature dependences of the heat capacity and entropy for these compounds are similar; to save space, we will compare the calculated and experimental results for the $Dy_2Ti_2O_7$ compound [13]. Figures 7 and 8 show the calculated and experimental temperature dependences of heat capacity and entropy for different values of external field H. For determining energy ε, we superimposed the temperatures of the calculated and experimental heat capacity peaks in zero external field ($H = 0$) (see Fig. 7a). The value of ε turned out to be 3 K, which is approximately 1.5 times smaller than the value of $\varepsilon \approx 4.35$ K obtained in [15] from an analysis of the temperature dependence of the density of monopole states in this compound. It can be seen from the figure that the calculated and experimental dependences of the thermodynamic functions (namely, the emergence of additional low-temperature anomaly in the temperature dependence of heat capacity for a certain value of field H; $H_{exp} = 0.75$ T and $H_{calc} = 1.5$ T) and the shift of this anomaly towards higher temperatures upon an increase in the value of H, as well as the decrease in the residual entropy upon an increase in the applied field H, are in good (at least, qualitative) agreement.

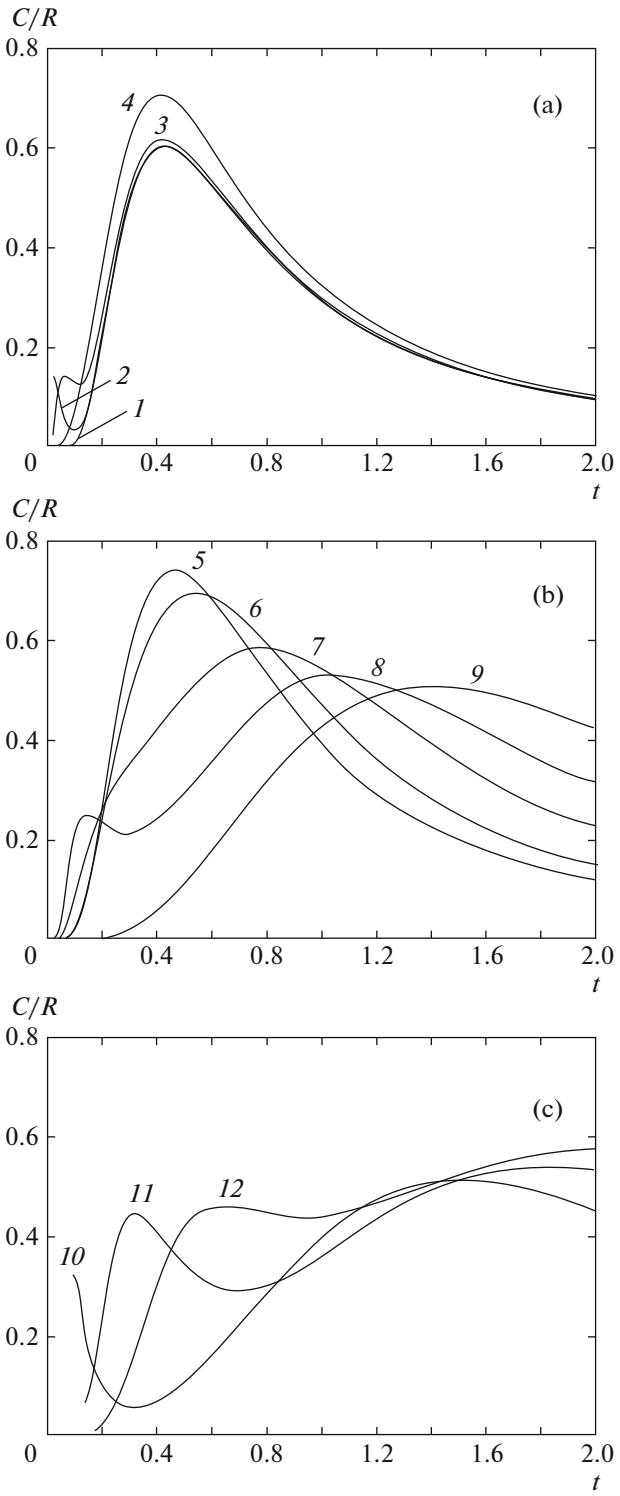

Fig. 4. Temperature dependences of heat capacity for different values of the external field: (a) $h = 0$ (*1*), 0.01 (*2*), 0.03 (*3*), and 0.1 (*4*); (b) $h = 0.2$ (*5*), 0.3 (*6*), 0.5 (*7*), 0.7 (*8*), and 1.0 (*9*); (c) $h = 1.1$ (*10*), 1.5 (*11*), and 1.9 (*12*).

2. $S \neq 0$, $H = 0$.

In this case, the ground state of the system is not degenerate because one of the six states of each tetrahedron has the minimal energy in field S. The temperature dependences of the heat capacity and entropy for different values of staggered field $s = S/\varepsilon$ are shown in Figs. 9 and 10. For low values of field $s < 0.1$, the temperature dependence of heat capacity exhibits two anomalies. The first anomaly is associated with the excitation of spin ice states. With increasing field s, the peak of this anomaly increases and shifts sharply towards high temperatures; at $s \approx 0.1$, this anomaly merges with the second anomaly associated with the excitation of magnetically charged configurations. The second anomaly in the temperature dependence

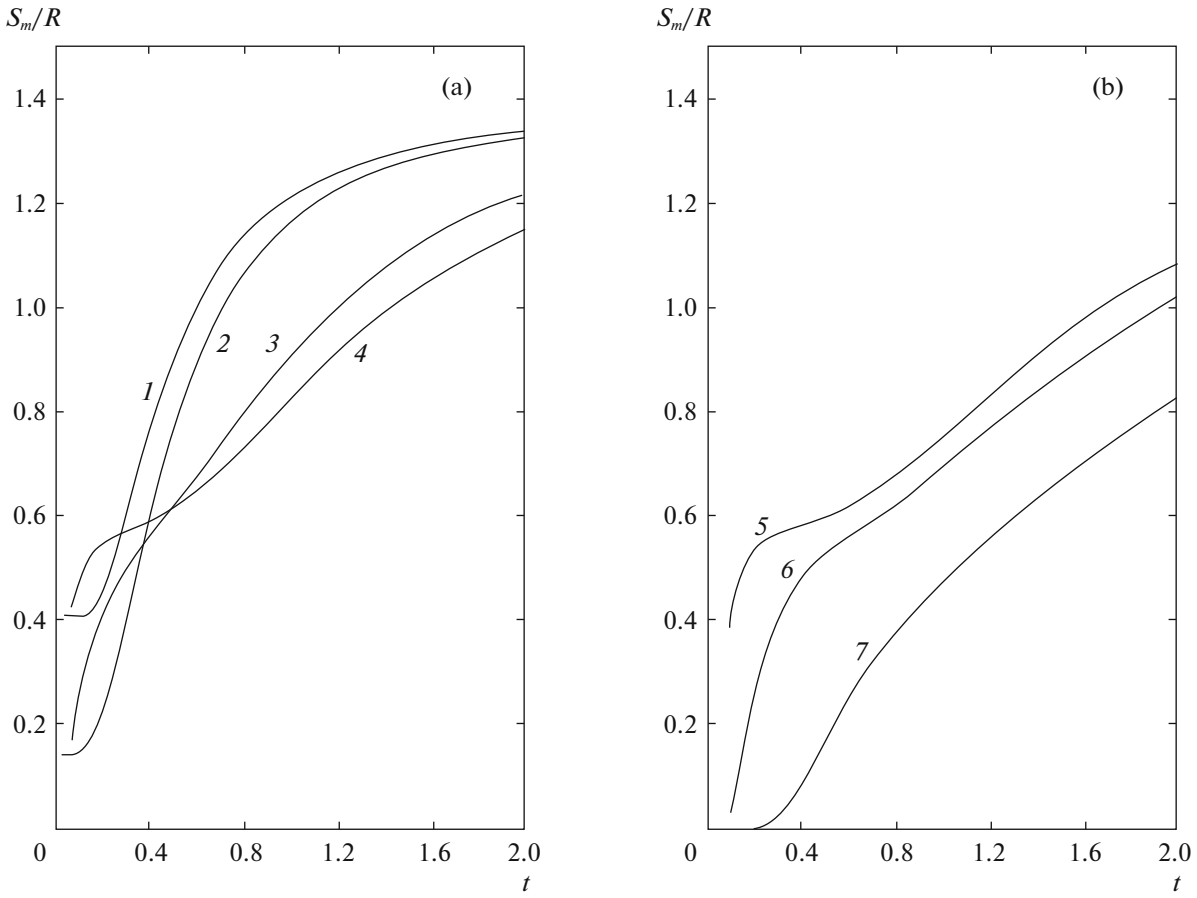

Fig. 5. Temperature dependences of entropy for different values of the external field: (a) $h = 0$ (*1*), 0.2 (*2*), 0.7 (*3*), and 0.9 (*4*); (b) $h = 1.1$ (*5*), 1.3 (*6*), and 1.9 (*7*).

of heat capacity is blurred upon an increase in field s, and its peak is shifted towards higher temperatures (see Fig. 9). The entropy for all nonzero values of s tends to zero as $T \to 0$ (see Fig. 10).

3. $S \neq 0$, $H \neq 0$.

Figure 11 show the temperature dependence of heat capacity for several values of s and h. It can be seen that with increasing staggered field as well as direct field, the anomalous dependence of the heat capacity is blurred, and its peak is shifted towards higher temperatures.

The case with $S \neq 0$ and $H \neq 0$ is typical of compounds of rare-earth oxides with the chalcolamprite structure, in which B^{4+} is a magnetic ion; in particular, $Pr_2Ru_2O_7$ [7], $R_2Ru_2O_7$ (R = Gd–Yb) [8], $Ho_2Os_2O_7$ [9], etc. The behavior of the heat capacity at low temperatures, including the case of a nonzero external field H, was studied experimentally for several compounds [7–9]. We will compare our results with experimental data obtained for $Pr_2Ru_2O_7$ compound. In this compound, a phase transition to the antiferromagnetic state, which is associated with ordering of magnetic moments of ruthenium, occurs at $T_N = 162$ K [7]. At low temperatures, the temperature dependences of heat capacity and entropy exhibit anomalies.

Figure 12 shows experimental temperature dependences of the low-temperature heat capacity [7] and the dependences calculated in this study for several values of direct field H in $Pr_2Ru_2O_7$. We have used the same value of the energy ($\varepsilon = 3$ K) of charged magnetic configurations and the value of staggered field $S = 1.5$ K as for $Dy_2Ti_2O_7$. It can be seen from Fig. 12 that the calculated $C(T)$ dependences correctly describe the experimental data qualitatively. The quantitative discrepancy between the calculated and experimental data is due to the fact that the experimental results apparently contain the lattice contribution to the heat capacity.

Unfortunately, we could not find experimental data on the low-temperature entropy for $Pr_2Ru_2O_7$ in the literature. The low-temperature behavior of entropy for $H = 0$ was investigated experimentally for $R_2Ru_2O_7$ (R = Gd–Yb) in [8]. A comparison of the entropy calculated in our study (for staggered field $S =$ 1.5 K) with the experimental dependences of entropy for $Yb_2Ru_2O_7$ is illustrated in Fig. 13. As noted above,

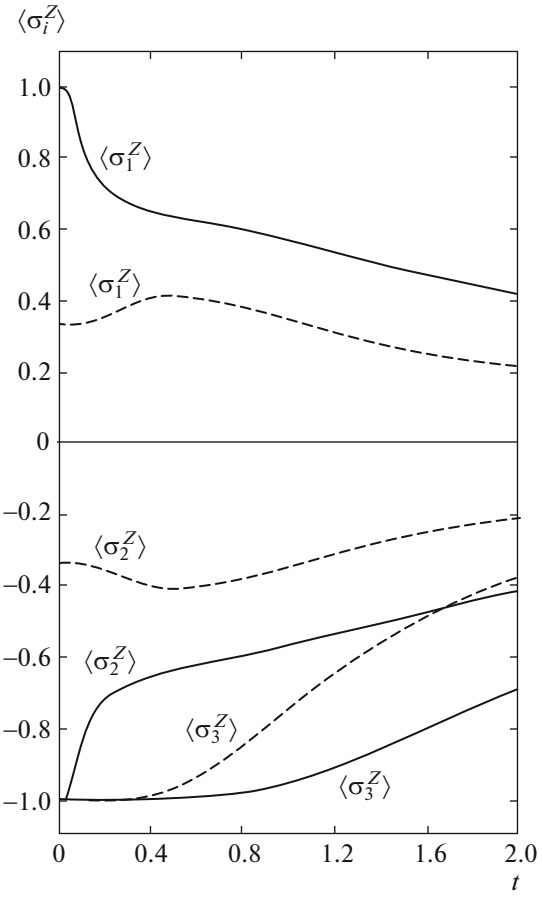

Fig. 6. Temperature dependences of mean values $\langle\sigma_i^Z\rangle$ for external field $h = 0.5$ (dashed curves) and $h = 1.1$ (solid curves), $\langle\sigma_2^Z\rangle = \langle\sigma_4^Z\rangle$.

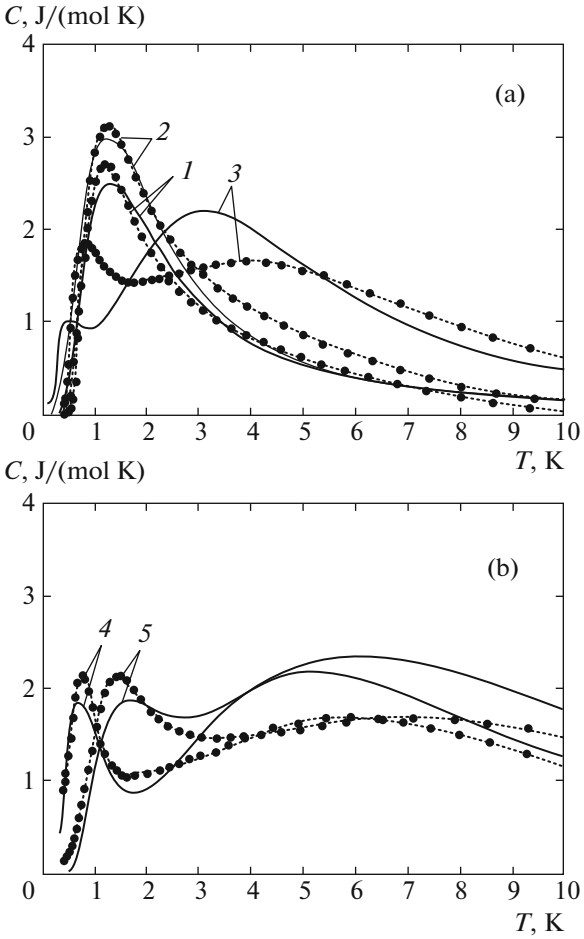

Fig. 7. Temperature dependences of heat capacity calculated in this study (solid curves) and experimental dependences for $Dy_2Ti_2O_7$ [13] (bullets) for different values of external field: (a) $H = 0$ (*1*), 0.25 T (*2*), and 1.5 T (*3*); (b) $H = 3$ T (*4*) and 4 T (*5*).

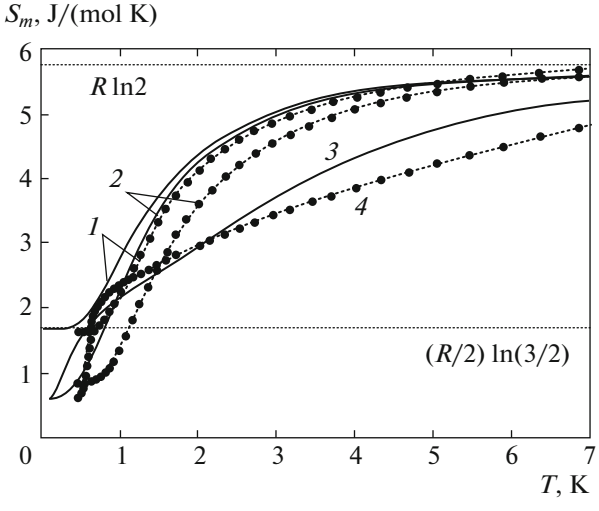

Fig. 8. Temperature dependences of entropy calculated in this work (solid curves) and obtained experimentally for $Dy_2Ti_2O_7$ [13] (bullets) for different values of external field: $H = 0$ (*1*), 0.25 T (*2*), 1.6 T (*3*), and 1 T (*4*).

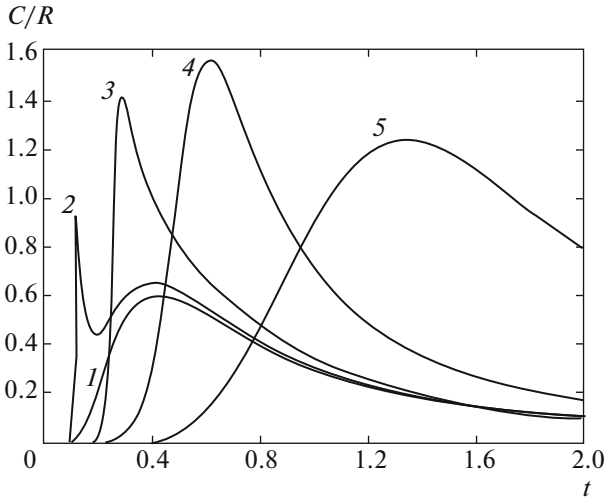

Fig. 9. Temperature dependences of heat capacity for different values of staggered field: $s = 0$ (*1*), 0.04 (*2*), 0.1 (*3*), 0.3 (*4*), and 1 (*5*).

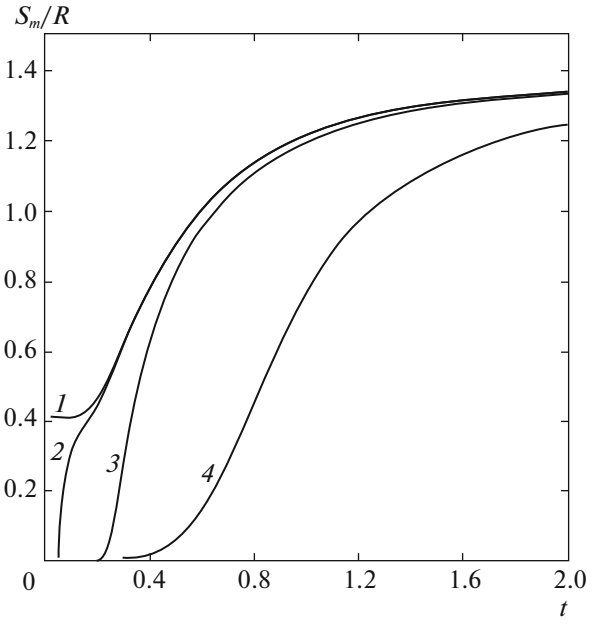

Fig. 10. Temperature dependences of entropy for different values of staggered field: $s = 0$ (*1*), 0.02 (*2*), 0.1 (*3*), and 0.5 (*4*).

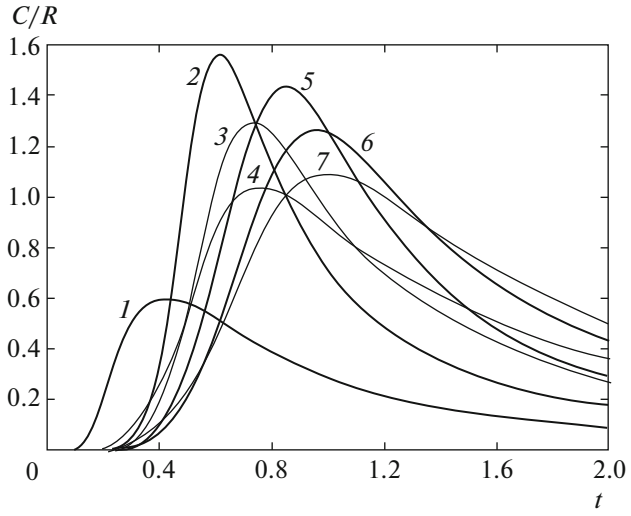

Fig. 11. Temperature dependences of heat capacity for different values of staggered and external fields: $s = 0$, $h = 0$ (*1*); $s = 0.3$, $h = 0$ (*2*); $s = 0.3$, $h = 0.3$ (*3*); $s = 0.3$, $h = 0.5$ (*4*), $s = 0.5$, $h = 0$ (*5*); $s = 0.5$, $h = 0.3$ (*6*), and $s = 0.5$, $h = 0.5$ (*7*).

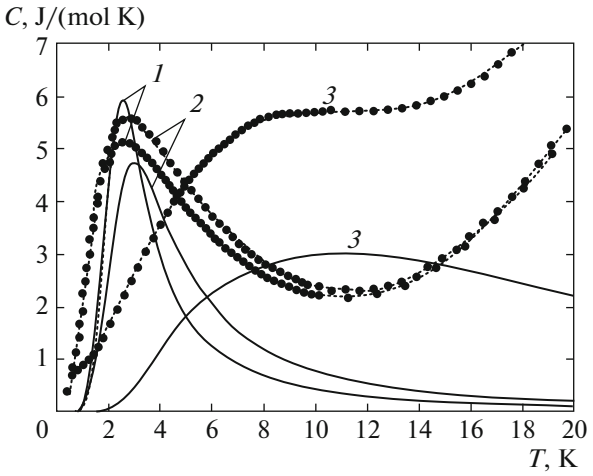

Fig. 12. Temperature dependences of heat capacity calculated in this work (solid curves) and obtained experimentally for $Pr_2Ru_2O_7$ [7] (bullets) for different values of external field: $H = 0$ (*1*), 1 T (*2*), and 9 T (*3*).

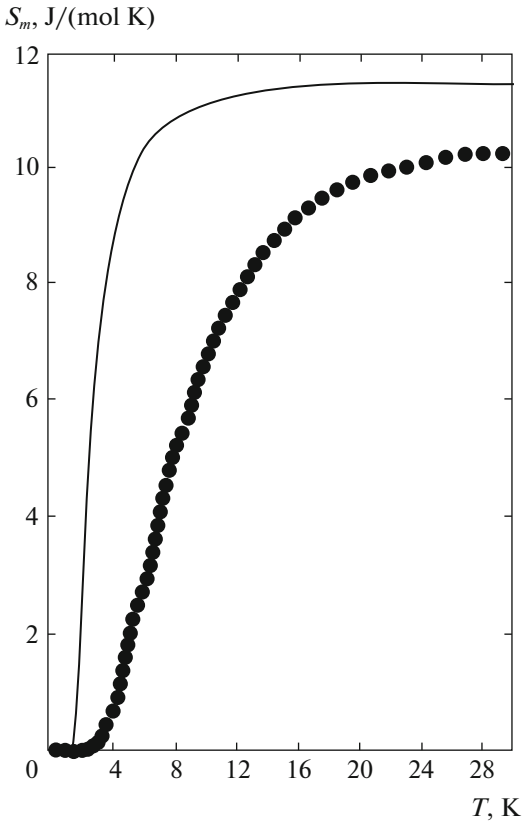

Fig. 13. Temperature dependences of entropy calculated in this work (solid curves) and obtained experimentally for $Yb_2Ru_2O_7$ [8] (bullets) for $H = 0$.

in the presence of staggered field, the calculated entropy of a system of magnetic moments of rare-earth ions tends to zero, which is confirmed experimentally.

4. CONCLUSIONS

In this study, we have investigated the low-temperature thermodynamic properties of spin ice in the staggered and direct (acting along the [111] axis) fields

in compounds of rare-earth oxides with general formula $Re_2^{3+}Me_2^{4+}O_7^{2-}$ with the chalcolamprite structure. The thermodynamic functions have been calculated in the cluster approximation using the smallest cluster of four particles, taking into account the spin ice state and magnetically charged states in the system of magnetic moments of ions of rare-earth elements. It has been found that the calculated temperature dependences of heat capacity and entropy are in good (at least qualitative) agreement with the experimental dependences. In particular, compounds with a nonmagnetic Me^{4+} ion (e.g., $Dy_2Ti_2O_7$) in an external field applied in the [111] direction exhibit one or two anomalies in the behavior of heat capacity (depending on the magnitude of this field); at $T \to 0$, residual entropy exists, the value of which decreases upon an increase in the external field. For compounds that contain a magnetic Me^{4+} ion, the staggered field produced by the antiferromagnetic ordering of the magnetic moments of Me^{4+} ions at the rare-earth ions leads to a nondegenerate ground state of the magnetic system of Re_2^{3+} ions and, as a consequence, to zero entropy at $T \to 0$. The low-temperature behavior of the heat capacity is also sensitive to the value of the field applied in the [111] direction (albeit to a smaller extent as compared to the case of compounds with a nonmagnetic Me^{4+} ion); this follows from a comparison of the calculated and experimental data for $Pr_2Ru_2O_7$ compound.

ACKNOWLEDGMENTS

This work was supported by the Russian Foundation for Basic Research, the Government of the Krasnoyarsk Territory, and the Krasnoyarsk Territory Foundation for Supporting the Scientific and Research Activity (project no. 16-42-243039).

REFERENCES

1. M. J. Harris, S. T. Bramwell, D. F. McMorrow, et al., Phys. Rev. Lett. **79**, 2554 (1997).
2. A. P. Ramirez, A. Hayashi, R. J. Cava, et al., Nature **399**, 333 (1999).
3. S. T. Bramwell and M. J. P. Gingras, Science **294**, 1495 (2001).
4. M. J. P. Gingras, in *Introduction to Frustrated Magnetism,* Ed. by C. Lacroix, P. Mendels, and F. Mila (Springer, Berlin, 2011), p. 293.
5. L. D. C. Jaubert, J. T. Chalker, P. C. W. Holdsworth, et al., Phys. Rev. Lett. **100**, 0672007 (2008).
6. P. N. Timonin, J. Exp. Theor. Phys. **113**, 251 (2011).
7. M. Tachibana, Y. Kohama, T. Atake, et al., J. Appl. Phys. **101**, 09D502 (2007).
8. N. Taira, M. Wakeshima, and Y. Hinatsu, J. Mater. Chem. **12**, 1475 (2002).
9. Z. Y. Zhao, S. Calder, and A. A. Aczel, Phys. Rev. B **93**, 134426 (2016).
10. E. H. Lieb and F. Y. Wu, in *Phase Transitions and Critical Phenomena,* Ed. by C. Domb and M. Green (Academic, New York, 1972), Vol. 1.
11. V. G. Vaks, *Introduction to the Microscopic Theory of Ferroelectrics* (Nauka, Moscow, 1973), p. 120 [in Russian].
12. L. Pauling, J. Am. Chem. Soc. **57**, 2680 (1935).
13. Z. Hiroi, K. Matsuhira, and S. Takagi, J. Phys. Soc. Jpn. **72**, 411 (2003).
14. H. D. Zhou, C. R. Wiebe, and J. A. Janik, Phys. Rev. Lett. **101**, 227204 (2008).
15. C. Paulsen, S. R. Giblin, and E. Lhotel, Nat. Phys. (2016). doi 10.1038/nphys3704

Translated by N. Wadhwa